Received 28 July 2020; revised 17 August 2020; accepted 25 August 2020. Date of publication 28 August 2020; date of current version 16 September 2020.

Digital Object Identifier 10.1109/OJAP.2020.3020239

Terahertz Antenna Array Based on a Hybrid Perovskite Structure

ABDOALBASET ABOHMRA [1] (Student Member, IEEE), HASSAN ABBAS [1,2] (Member, IEEE), MUATH AL-HASAN [3] (Senior Member, IEEE), ISMAIL BEN MABROUK [3] (Senior Member, IEEE), AKRAM ALOMAINY [4] (Senior Member, IEEE), MUHAMMAD A. IMRAN [1,2] (Senior Member, IEEE), AND QAMMER H. ABBASI [1,2] (Senior Member, IEEE)

[1]James Watt School of Engineering, University of Glasgow, Glasgow G12 8QQ, U.K.

[2]Jams Watt School of Electronic Engineering, University of Glasgow, Glasgow G12 8QQ, U.K.

[3]College of Engineering, Al Ain University Abu Dhabi, Abu Dhabi, UAE

[4]School of Electronic Engineering and Computer Science, Queen Mary University of London, London E1 4NS, U.K.

CORRESPONDING AUTHOR: A. ABOHMRA (e-mail: 2356006a@student.gla.ac.uk)

This work was supported in part by ADEK Award for Research Excellence under Grant AARE19-245, and in part by the University of Glasgow through Engineering and Physical sciences Research Council (EPSRC) under Grant P/R511705/1. Authors would like to thank the Government of Libya for providing funding for the doctoral studies.

ABSTRACT This article presents a novel terahertz (THz) antenna array design comprising a layered structure of a perovskite material which enhances the radiation characteristics of an antenna overlaid on a conventional metallic antenna element. The simulated antenna consists of a THz gold patch antenna coated with a hybrid perovskite material, methyl-ammonium lead iodide $CH_3NH_3PbI_3$ which enables the manipulation of the THz electromagnetic waves. In addition to this, we also present a comparison of the antenna properties of the proposed hybrid perovskite material with antennas made of gold and perovskite only. The proposed antenna operates in the frequency band 0.9 - 1.2 THz. The simulated impedance bandwidth of the proposed array antenna ranges from 0.9 THz to 1.2 THz with a reflection coefficient (S11) less than −10 dB. The antenna array has a radiation patterns stability on the whole frequency band. The peak gain obtained is 11.4 dBi with perovskite arrays. The hybrid and perovskite antenna array demonstrate high radiation efficiency. The designs presented here will help in realising future wireless communication systems that require miniaturisation, fast reconfigurability and wearability.

INDEX TERMS Perovskite, gold, terahertz, antenna.

I. INTRODUCTION

THERATZ radiation is the electromagnetic spectrum lactated between the optical and microwave frequency band from 0.1 to 10 THz [1], [2]. It combines the benefits of these two regions, as well as its non-ionising radiation, high resolution, and sufficient penetration into nonconducting materials [3]. In comparison with the optical, infrared, and microwave devices, THz wave systems are relatively unexplored, and the related technology is still in its early stages [4]. For short-range wireless communication, THz shows significant potential in the development of wireless communication systems that can meet the increasing demands of high bandwidths and data rates and therefore, overcome the communication channel bottlenecks [5], [6]. However, one major concern in the usage of the THz spectrum for short-range wireless communications is the atmospheric attenuation [7]. Recently, advancements in the design and development of antennas have been made using fabrication techniques such as electron beam lithography which require high throughput device fabrication methods [8]. This type of technology can fabricate devices at the nanoscale, ideal for plasmonic antennas [9]. Even though, THz band in the close to millimeter frequency of the electromagnetic range is promising yet before the marketing, the related challenge of the THz system configuration ought to be addressed. The atmospheric effect is the fundamental

challenge to the THz commercial implementation [10]. To conquer this problem, the transmission power and efficiency of detection should be increased. The power source can be expanded to just a specific degree and the yield intensity of the greater part of the power is confined to milli-watt extend. Because of this restriction of the sources, the function of transmitting and receiving antenna at THz band became significantly important [11]. The yield power is comparing to the square of the partition between the accepting and transmitting radio wire. Consequently, it is essential to enhance the gain of the antenna in the THz band to propagate the signal to wide extension [12]. Recently, various THz nanoantenna arrays for THz application have been proposed. Dipole nanoantennas assurance to significantly improve the abilities of THz spectroscopy, offering the opportunity of extending its affectability through near field enhancement [13]. Examination the light coupling property of thick array of sub-wavelength THz antenna microcavities in [14] with simple structures. A scalable 4×4 array power generator and scanning introduced in [15] and W frequency band direct detection based receiving array is presented in [16] utilizing another idea of spatial-overlapping for mm-wave imaging application. A simulated design of 16 element antenna array at 0.3 THz has been presented in [17] the antenna array achieved maximum directivity of 18.1 dBi. Aside from the microstrip antenna, the Yagi–Uda antenna has been utilized for THz wireless communication [18]. Alternatively, patch antenna array have the advantage of low profile, low cost and easy to fabricate despite of having narrow transmission capacity [19]. However, THz antennas array cannot be accomplished by just reducing the metal antenna dimensions to a few micrometres [20]. This is because of the low mobility of electrons in the metal nano structure, which would incur a high channel attenuation and therefore prevent nano-transceivers from working properly [21]. Most antenna radiation metals are copper, sliver and aluminium. The utilization of metals is conducted by the desire of high electrical conductivity for transmitting and receiving. However, the radiation from these metals is limited by the skin depth and the intrinsic property at THz frequency. As conductor loss becomes progressively restrictive at higher frequencies, metamaterials have emerged as attractive candidates providing a wide scope of material properties [22]. The skin depth is a helpful method to distinguish the area of the conductor where the most of the current flows. It becomes not useful to utilise a conductor with a radius more than the skin depth regardless of the transmitter size [23]. In the case of traditional materials, the extremely small size combined with the prohibitively high resistance per unit length restricts usage in THz applications such as essentially electrical interconnects and radiating patches. The conventional material skin depth effect is given by [23],

$$\delta = \sqrt{\frac{\rho}{\pi f \mu_r \mu_0}} \tag{1}$$

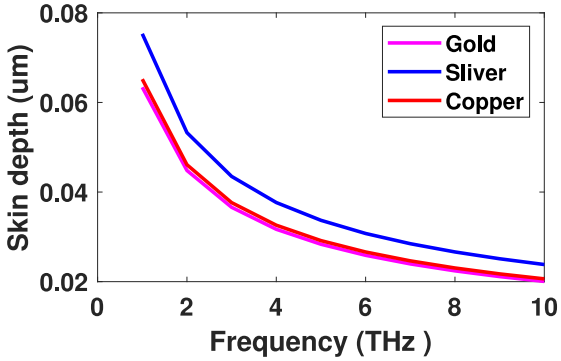

FIGURE 1. The skin depth of three different metals (Gold,Sliver and Copper) at the THz frequency band.

where δ is the skin depth, ρ is the resistivity, f is the signal frequency, μ_r relative permeability and μ_0 is the permeability of free space. Figure 1 demonstrates that the skin depth reduces with the rising in the working frequency. The skin depth of conventional conductor materials in the THz band is several hundred nanometres. Gold (Au) shows smaller skin depth than other metals (copper (Cu), and silver (Ag)). Also, the surface resistivity of conventional metal increments with the frequency because of the skin impact and thus the radiation efficiency of nanoantenna becomes extremely low, because of the high ohmic losses at such small sizes [24].

The THz conductivities of Ag, Au, and aluminium (Al) thin films were measured using the transmission response in [25]. Results show that the thinner films have less conductivity and vice versa. This reduced conductivity can be attributed to a large scattering carrier as a result of lattice faults in the conductor at THz frequencies [26]. To tackle the skin depth challenges, replacement materials like graphene has been researched in the field of wireless communication applications [27]. These materials must be easily fabricated, therefore can be coated as a film. Alternative two-dimensional (2D) materials, for instance, the Molybdenum disulfide (MoS_2), were investigated for fabrication of devices functioning in the THz region [28]. Despite interesting property of these materials, the theoretical understanding of these materials stays limited. Among all famous 2D materials, the perovskite $CH_3NH_3PbI_3$ material films has proven a good performance in many THz applications.

A. PEROVSKITE MATERIALS

Perovskites are materials expressed using a chemical formula of ABX_3, where A and B are cations of different sizes and X is an anion [29]. Their crystallographic stability and proper structure can be found through the consideration of the tolerance factor t characterized as the proportion of the separation A−X to the separation between B−X in an idealised solid sphere model and the octahedral factor χ [30]. For halide perovskites where X = F_2, Cl_2, Br_2, I_2, t generally ranges from 0.81 - 1.11 and χ between 0.44 - 0.90. If t lies in smaller range 0.89 - 1.0, the cubic structure of Fig. 2

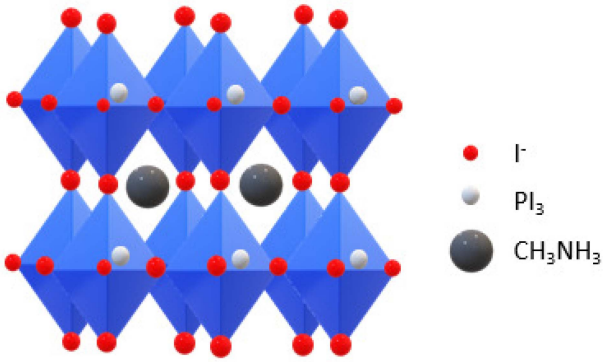

FIGURE 2. The crystal structure of $CH_3NH_3PbI_3$ perovskite. It consists of a framework of comer-sharing lead (grey) halide (red) octahedrals.

is predicted that, with lower tolerance will permit a small symmetric tetragonal or orthorhombic configuration [31].

Organic-inorganic halide perovskites have recently attracted interest, particularly as the larger cation A is organic, it is broadly methylammonium (CH_3NH_{3+}). Current researches aims have concentrated on overcoming the propagation problems at THz band by developing efficient sources and antennas [32]. Hence, THz antenna can now be found in many THz application such as biomedical sensing, imaging and short-extend wireless communication [33]. The real part of the perovskite conductivity increases with frequency, while the imaginary part is negative at low frequencies and starts to increase at higher frequencies [34], [35]. Figure 3(a) shows the dielectric permittivity of $CH_3NH_3PbI_3$ at 300 K. The real part of the dielectric constant is seen increasing with frequency in the THz band; it is 30 at 0.1 THz and reaches 55 at 10 THz, while the imaginary part is close to 0 from 1 - 10 THz as shown in Fig. 3(b). An efficient THz gadget is basic in building up a high performance THz system, carbon materials has been revealed promise in THz application [36], [37]. THz frequency antennas, devices, and detectors based on new materials have only been designed and evaluated theoretically so far. Also, numerical simulations are limited in terms of presenting a complete design [27], [38]. Also, perovskite antenna structures require complex fabrication processes due to a dry etching process and the need to transform the perovskite film on to a substrate and biasing networks to control material properties and improve its performance. However, substantial progress has recently been made due to improvements in fabrication techniques that pave the way to realise nanoscale perovskite structures. On the other hand, perovskites, because of property, for example, superconductivity, ferroelectricity, and cost-effective, have picked up consideration in various THz applications [39]. The material is therefore, attractive in developing high efficiency systems in the THz and infrared frequency bands [40], [41]. Perovskites have been broadly inspected given their appealing electronic properties and thus have found applications in photovoltaics [31], [34]. Perovskites have also been studied in terms of realising superconductivity, ferroelectricity, and excessive thermopower [35]. The extent of exploration of ferroelectric and superconductor constructions can be a combination of high-temperature superconductors and ferroelectric films for growing novel digital devices [42]. In [43], an experimental demonstration of $CH_3NH_3PbI_3$ based energetic manipulation of Fano resonances in a perovskite metamaterial system is discussed, whereby the photoexcitation of perovskite layer spin covered on the metamaterial shape actively modulates and switches off the Fano resonance characteristic in the THz asymmetric split ring resonator was presented. Similarly, in [44] a tremendous overall performance of solution prepared $CH_3NH_3PbI_3$ film as a stage for an ultrafast all optical trade incorporated with a flexible meta device. A single step spin-coating methodology of the perovskite film permits a passive metal gadget acquire the progressively tuneable photoconductivity from the perovskite layer hence, permits the flexible hybrid metaphotonic system that carries on as a functioning ultrafast, low threshold optical switch. In [45], a simple yet ultrafast THz photonic machine through integrating two-dimensional (2D) perovskites with the THz metamaterial for superior manipulation of THz waves. The existence of (quantum wave structures) in the 2D perovskite thin film provides steady excitons at room temperature via localised photoexcited free carriers in quantum waveguides leads to ultrafast systems. In other studies [46], highly confined plasmon-induced transparency enabled a high-energy manipulation of photons with high sensitivity. The embedded semiconducting materials utilised spin-covered perovskite films which performed as a photo energetic medium to endow the system with high sensitivity and ultrafast velocity an anisotropic THz energetic metamaterial system. The interesting probability is that, $CH_3NH_3PbI_3$ perovskite could have paraelectric and ferroelectric at 300k, improving the performance at THz [47]. The fundamental evidences for this is the hysteresis distinguished in resistivity assessment, which is not seen in related structure prepared similarly, and the rest of polarization is apparent as a limited voltage yield at zero current [48]. The crystallographic point gathering (4mm) of both the 300k and higher iodide stages is steady with ferroelectric conduct [49]. Hysteresis has likewise been accounted for high-proficiency gadgets, however different clarifications are additionally potential for this other than ferroelectric impacts [48], [49].

B. PATCH ANTENNA ARRAY DESIGN

For designing a THz microstrip patch antenna, we explain the antenna parameters, based on the operating frequency and the material properties. The width of the antenna is calculated by, [50],

$$W \approx \frac{c_0}{2f_r}\sqrt{\frac{2}{\varepsilon_r + 1}} \tag{2}$$

where w is the width of the patch, c_0 the speed of light, f_r the resonant frequency, and ε_r the dielectric constant of the

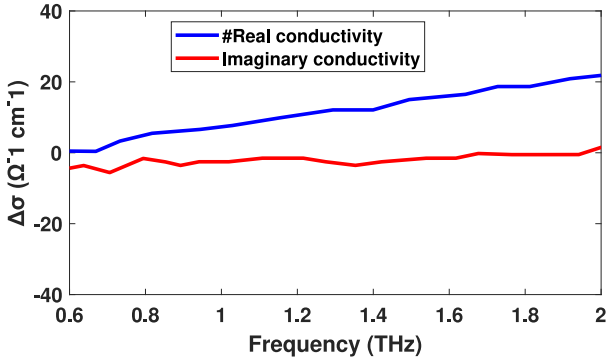

(a) The electrical conductivity of $CH_3NH_3PbI_3$ at 300 K [32].

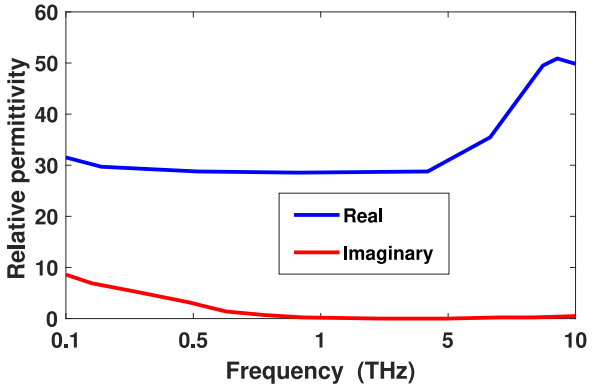

(b) The relative permittivity of $CH_3NH_3PbI_3$ at 300 K [33].

FIGURE 3. The electrical properties of perovskite.

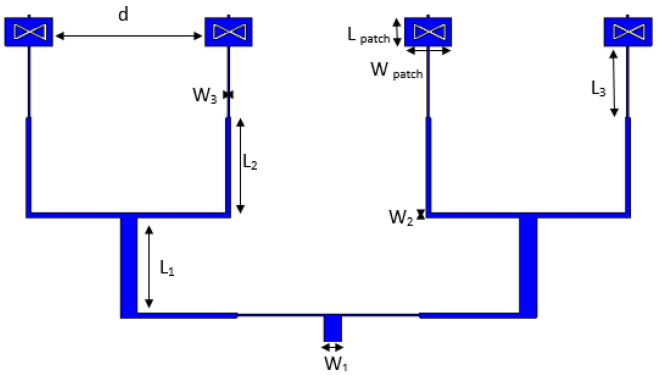

(a) Portion of the array feed network of the proposed antenna illustrating the voltage divider network (50Ω 70Ω 100Ω).

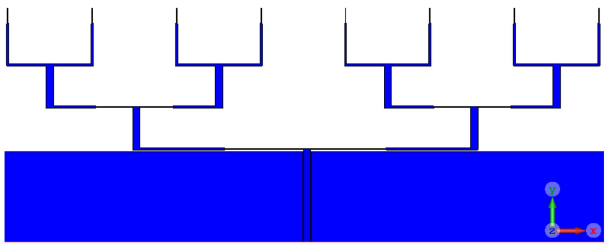

(b) The designed ground-signal-ground type coplanar waveguide (CPW) and the feeding network optimized using CST optimization tool

FIGURE 4. The feed lines dimensions of the antenna array.

substrate. The effective permittivity (ε_{eff}) of a patch element of height h is normally used in the antenna design as it takes into account the fringe electric fields,

$$\varepsilon_{eff} = \frac{\varepsilon_r + 1}{2} + \frac{\varepsilon_r - 1}{2}\left[\frac{1}{\sqrt{\frac{1}{1+12\frac{h}{w}}}}\right]. \quad (3)$$

Due to the fringing, the electrical size of the antenna is increased by an amount of ΔL, which can be found using [32],

$$\frac{\Delta L}{h} = 0.412\frac{(\epsilon_r ff + 0.3)\left(\left(\frac{W}{h}\right) + 0.264\right)}{(\epsilon_r ff + 0.258)\left(\left(\frac{W}{h}\right) + 0.8\right)} \quad (4)$$

The effective length of the antenna patch can be determined by,

$$L_{eff} = L + 2\Delta L \quad (5)$$

In a microstrip array having a large number of antenna elements, the feeding network is essential in obtaining a high antenna gain. The feeding network designed using transmission line theories controls the amplitude, as well as the phase of the current, supplied to each antenna element. The feed line dimensions (width and length) required to obtain 50, 70, and 100 Ω antenna array input impedance at the desired frequency are [51],

$$Wf = 7.48 \times h\exp\left(-Z_0\frac{\sqrt{\varepsilon_r + 1.41}}{87}\right) - 1.25 \times t. \quad (6)$$

Here Wf is the line width, Z_0 is the input impedance, and t is the trace thickness. Similarly, the feed line length L can be calculated using,

$$L_t = (2M + 1) \times \lambda \quad (7)$$

where M is an integer and λ is the wavelength.

The hybrid antenna design proposed in this article is simulated and analysed using a full-wave commercial electromagnetic solver (CST Microwave Studio 2020). Figure 4 and Table 1 illustrate the parameters for the feeding network of the antenna array operating in the 0.9 - 1.2 THz band calculated using (6) and (7). The values are obtained so that the feed is matched with the resonant antenna element. Because of the amplitude and phase of the radiated fields at each patch are dictated by the total transmission qualities of the previous patches on the line, the patches should be optimised in order to accomplish a desired amplitude and phase

TABLE 1. The dimensions in μm of the feed lines network.

Dimension	Size extension (μm)
W_{patch}	70
L_{patch}	119
W_1 (50Ω)	43
W_2 (70Ω)	12
W_3 (100Ω)	4
L_1	250
L_2	250
L_3	180
d	350

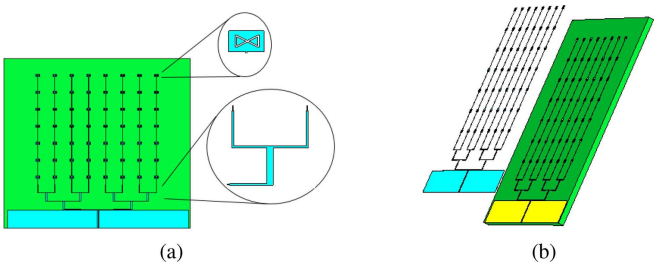

FIGURE 5. The proposed antenna design: (a) Front profile of the antenna; (b) antenna structure (perovskite and gold layer).

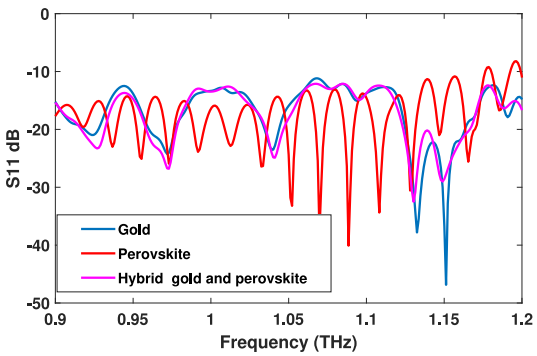

FIGURE 6. The simulated S11 of the antennas array.

distributions of transmitting currents along the structure. The array design contains 57 elements on a 5 mm × 5 mm substrate (Figs. 5(a) and 5(b)). The feeding network has been optimised using the optimisation tool found in the CST environment. In order to reduce the effect of mutual coupling, the distance d is kept greater than $\lambda/2$. Figure 5(b), 5(a) shows the antenna consisting of $CH_3NH_3PbI_3$ perovskite, gold, and a Polyethylene naphthalate polyethylene naphthalene (PEN) substrate, which is one of the transparent and flexible substrates, commonly used in the development of flexible electronics. PEN offers a good resistance to chemical solvents and a discrete acceptance to high temperature [52]. The thin flexible Polyethylene naphthalate PEN film is used as a substrate with a consistent dielectric constant of $\varepsilon_r = 2.5$ and loss tangent $\tan\alpha = 0.00025$ in the operating frequency range.

II. RESULTS AND DISCUSSION

Figure 6 shows that the antenna operates well in an ultra-wideband frequency range of 0.9 to 1.2 THz. The figure

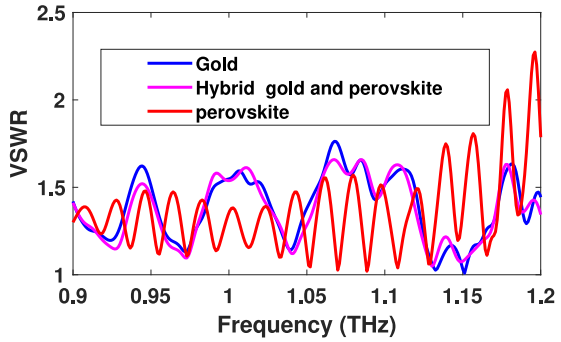

FIGURE 7. Antenna VSWR in the operating frequency range.

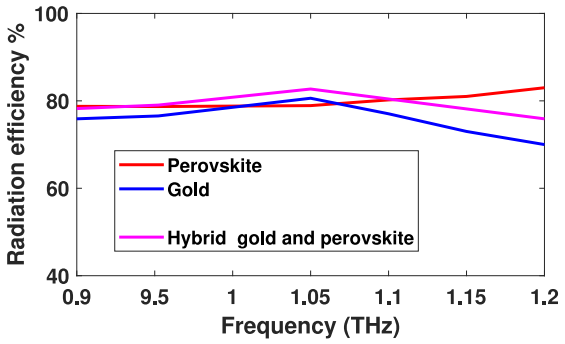

FIGURE 8. The radiation efficiency of the three materials shown separately.

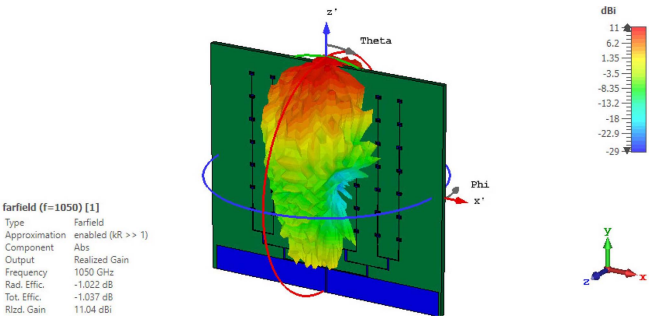

FIGURE 9. 3D radiation pattern.

shows that the simulated reflection coefficient in the desire frequency range from 0.9 - 1.2 THz. The perovskite material separately as well in a hybrid combination with gold provides an excellent antenna performance in the desired frequency range. On the other hand, the antenna performance of antenna based gold material failed to achieve the −10 dB reflection coefficient at frequencies above 1.15 THz as compared to gold, perovskite materials have significantly higher conductivity which leads to better antenna reflection. Figure 7 shows that the VSWR remains below 2 throughout the targeted frequency band, which demonstrates an excellent impedance matching.

The radiation efficiency of the antenna is shown in Fig. 8. Despite the decrease in the radiation efficiency at 1.05 THz, the antenna still achieves a high radiation efficiency above 83% with both perovskite and hybrid material designs. As the

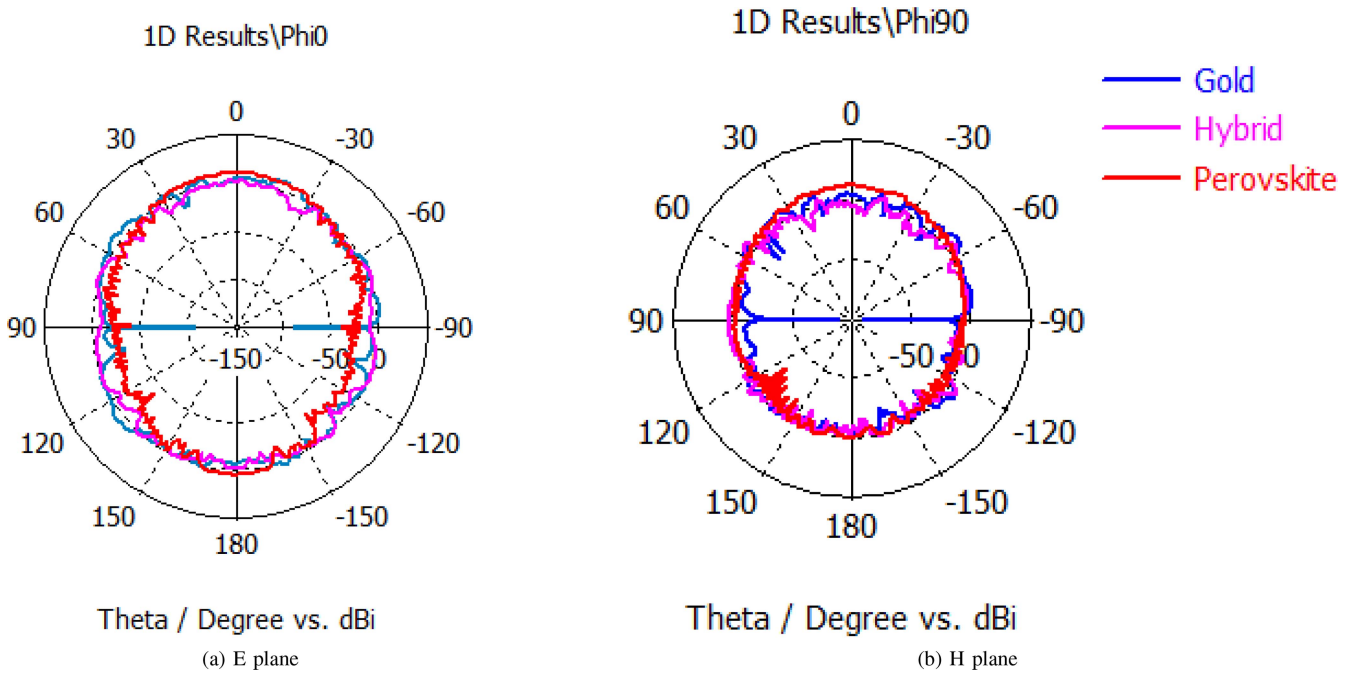

(a) E plane (b) H plane

FIGURE 10. Radiation patterns, (a) E-plane, (b) H-plane, (c) pattern at 1.05 THz.

conductivity of the perovskite increases with the frequency, the radiation efficiency is improved. The increasing of charge density enhancing the electric field which explain the efficiency enhancement across the operating frequency band by using perovskite material. The radiation efficiency of gold antennas is lower than perovskite and hybrid antenna array because of the related high ohmic loss at these small sizes, the efficiency of gold decrease with frequency above 1.05 THz due to high gold surface impedance. The gold antenna efficiency continues to drop until it reaches 65% at 1.2 THz. Whereas, the radiation efficiency of the perovskite material and the hybrid material structure (gold and perovskite) maintain an excellent radiation efficiency of 85% and 80% respectively. Both structures maintain a high efficiency within the target frequency band. Table 2 presents a comparison of the three propsed array performance and it can be seen that the overall performance is enhanced in terms of gain and directivity. The Table 2 shows an improvement in the gain and directivity, whereas the gain of hybrid antenna has increased by 11% without reduction in the bandwidth. The best result has been achieved with perovskite antenna, where the gain was achieved at 1.1 THz and it was 11.4 dBi and that is 21% higher than the gold array antenna, this percentage can be improved if external voltage is applied to increase the electrons density in perovskite film and consequently enhance the electric field further but at same time it make the design complicated as it needs a complete external biasing circuit. From Fig 9. shows the radiation direction towards the elevation angle due to the absence of ground plane (Un-grounded CPW) which mean there is no reflection from the back of the substrate. Thus, the reflection of radiation would be is towards the elevation angle. The

TABLE 2. Comparison of antenna arrays structures.

Antenna	Gain	Directivity
Gold	8.942 dBi	10 dBi
Hybrid antenna	10.13 dBi	11.3 dBi
Perovskite	11.4 dBi	12.05 dBi

radiation pattern of the transparent antenna at the 1.1 and 1.05 THz frequencies are presented in Figure 10(a), 10(b) and 11(a), 11(b) respectively. From the figures the E plane of the antenna is bidirectional though the H plane radiation pattern is nearly omnidirectional. The radiation pattern is stable and symmetrical within the desire band of the frequency. Due to the perovskite material reflection underneath the gold, ripples was observed in the radiation results. The radiation patterns of the three antenna array structures shows a high main lobe magnitudes with lower back lobes at 1.05 THz frequency (Figure 10(a) and 10(b)) and 1.1 THz (Figure 11(a) and 11(b)). 7.1 dBi main lobe was observed with gold material structure and increased with hybrid and perovskite antenna array, 10 and 12.1 dBi respectively. Consequently, more side lobe observed at gold antenna compared to hybrid and perovskite array. The patterns at selected frequency is not ideally broadside in the whole operating range, but this impact comes as a compromise when the antenna is designed to cover a large bandwidth. The high transmission capacity, high gain and efficiency declare that the usefulness of perovskites as an enhancement material to gold metal at THz band.

With these remarkable functional properties, perovskites provide new pathways for trending research in the field of antenna and reflectarray devices. Moreover, their properties

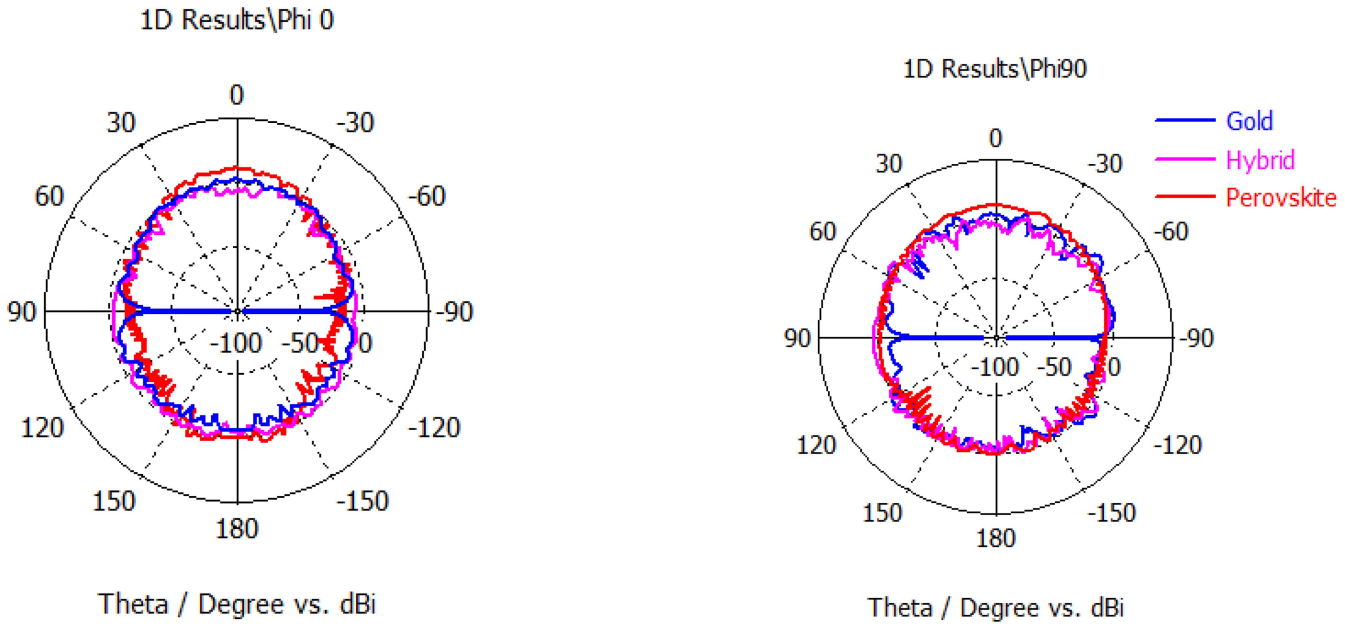

(a) E plane

(b) H plane

FIGURE 11. Radiation patterns: (a) E-plane, (b) H-plane at 1.1THz.

can be enhanced or exploited as an efficient THz device by integrating perovskite with conventional metal resonant structures such as gold or copper.

III. CONCLUSION

In this article, we showed a novel hybrid THz antenna array design made from gold and perovskite layers. The antenna array was simulated using a multi-layered structure of perovskite, gold, and PEN substrate. Results show that in the frequency range of 0.9 - 1.2 THz, the antenna performance significantly improves over a gold-only antenna. The proposed work also shows that with the fast emergence of 2D materials having electrical conductivity. The electrical properties can be controlled to a better performance by selecting the preparation method by chemical doping or external basing. The perovskite and hybrid antenna array display better performance at room temperature which is superior. The result open a way for more profound understanding and further improvement of perovskite material in various applications. The capacity to be a decent radiating element at room temperature is a remarkable feature which puts this materials in an exclusive class of supporting conventional metal at THz frequency band. The result shows that the $CH_3NH_3PbI_3$ is incredibly promising for advanced THz applications, particularly THz wireless communication. Future work would be concentrated on optimisation of the intrinsic property and fabrication methods of thin films for adoption in THz antenna.

REFERENCES

[1] S. Bhattacharjee *et al.*, "Folded waveguide traveling-wave tube sources for terahertz radiation," *IEEE Trans. Plasma Sci.*, vol. 32, no. 3, pp. 1002–1014, Jun. 2004.

[2] Q. Wu and X.-C. Zhang, "7 Terahertz broadband GaP electro-optic sensor," *Appl. Phys. Lett.*, vol. 70, no. 14, pp. 1784–1786, Apr. 1997.

[3] X.-C. Zhang and J. Xu, *Introduction to THz Wave Photonics*. New York, NY, USA: Springer, 2010.

[4] L.-H. Gao *et al.*, "Broadband diffusion of terahertz waves by multi-bit coding metasurfaces," *Light Sci. Appl.*, vol. 4, no. 9, pp. e324–e324, 2015.

[5] T. Kürner and S. Priebe, "Towards THz communications—Status in research, standardization and regulation," *J. Infrared Millim. Terahertz Waves*, vol. 35, no. 1, pp. 53–62, Jan. 2014.

[6] T. Kleine-Ostmann and T. Nagatsuma, "A review on terahertz communications research," *J. Infrared Millim. Terahertz Waves*, vol. 32, no. 2, pp. 143–171, Feb. 2011.

[7] T. Nagatsuma, G. Ducournau, and C. C. Renaud, "Advances in terahertz communications accelerated by photonics," *Nat. Photon.*, vol. 10, no. 6, pp. 371–379, Jun. 2016.

[8] C. W. Berry, N. Wang, M. R. Hashemi, M. Unlu, and M. Jarrahi, "Significant performance enhancement in photoconductive terahertz optoelectronics by incorporating plasmonic contact electrodes," *Nat. Commun.*, vol. 4, no. 1, p. 1622, Jun. 2013.

[9] S. S. Dhillon *et al.*, "The 2017 terahertz science and technology roadmap," *J. Phys. D, Appl. Phys.*, vol. 50, no. 4, Feb. 2017, Art. no. 043001.

[10] M. Koch, "Terahertz communications: A 2020 vision," in *Terahertz Frequency Detection and Identification of Materials and Objects*. Dordrecht, The Netherlands: Spriger, 2007, pp. 325–338.

[11] K. R. Jha and G. Singh, "Terahertz planar antennas for future wireless communication: A technical review," *Infrared Phys. Technol.*, vol. 60, pp. 71–80, Sep. 2013.

[12] F. Meshkati, H. V. Poor, S. C. Schwartz, and N. B. Mandayam. "An energy-efficient approach to power control and receiver design in wireless data networks," *IEEE Trans. Commun.*, vol. 53, no. 11, pp. 1885–1894, Nov. 2005.

[13] L. Razzari *et al.*, "Terahertz dipole nanoantenna arrays: Resonance characteristics," *Plasmonics*, vol. 8, no. 1, pp. 133–138, 2013.

[14] C. Feuillet-Palma, Y. Todorov, A. Vasanelli, and C. Sirtori, "Strong near field enhancement in THz nano-antenna arrays," *Sci. Rep.*, vol. 3, no. 1, pp. 1–8, 2013.

[15] K. Sengupta and A. Hajimiri, "A 0.28 THz power-generation and beam-steering array in CMOS based on distributed active radiators," *IEEE J. Solid-State Circuits*, vol. 47, no. 12, pp. 3013–3031, Dec. 2012.

[16] F. Caster, II, L. Gilreath, S. Pan, Z. Wang, F. Capolino, and P. Heydari, "Design and analysis of a W-band 9-element imaging array receiver using spatial-overlapping super-pixels in silicon," *IEEE J. Solid-State Circuits*, vol. 49, no. 6, pp. 1317–1332, Jun. 2014.
[17] R. Piesiewicz, M. N. Islam, M. Koch, and T. Kurner, "Towards short-rangeterahertz communication systems: Basic considerations," in *Proc. IEEE 18th Int. Conf. Appl. Electromagn. Commun.*, Dubrovnik, Croatia, 2005, pp. 1–5.
[18] D. Gray, J. W. Lu, and D. V. Thiel, "Electronically steerable Yagi–Uda microstrip patch antenna array," *IEEE Trans. Antennas Propag.*, vol. 46, no. 5, pp. 605–608, May 1998.
[19] K.-M. Luk *et al.*, "A microfabricated low-profile wideband antenna array for terahertz communications," *Sci. Rep.*, vol. 7, no. 1, pp. 1–11, 2017.
[20] W. Knap *et al.*, "Nonresonant detection of terahertz radiation in field effect transistors," *J. Appl. Phys.*, vol. 91, no. 11, pp. 9346–9353, Jun. 2002.
[21] W. Knap *et al.*, "Terahertz emission by plasma waves in 60 nm gate high electron mobility transistors," *Appl. Phys. Lett.*, vol. 84, no. 13, pp. 2331–2333, Mar. 2004.
[22] J. Lloyd-Hughes and T.-I. Jeon, "A review of the terahertz conductivity of bulk and nano-materials," *J. Infrared Millim. Terahertz Waves*, vol. 33, no. 9, pp. 871–925, Sep. 2012.
[23] A. K. Azad and W. Zhang, "Resonant terahertz transmission in subwavelength metallic hole arrays of sub-skin-depth thickness," *Opt. Lett.*, vol. 30, no. 21, pp. 2945–2947, Nov. 2005.
[24] G. Hanson, "Radiation efficiency of nano-radius dipole antennas in the microwave and far-infrared regimes," *IEEE Antennas Propag. Mag.*, vol. 50, no. 3, pp. 66–77, Jun. 2008.
[25] N. Laman and D. Grischkowsky, "Terahertz conductivity of thin metal films," *Appl. Phys. Lett.*, vol. 93, no. 5, Aug. 2008, Art. no. 051105.
[26] N. Laman and D. Grischkowsky, "Reduced conductivity in the terahertz skin-depth layer of metals," *Appl. Phys. Lett.*, vol. 90, no. 12, Mar. 2007, Art. no. 122115.
[27] Z. Li, K. Yao, F. Xia, S. Shen, J. Tian, and Y. Liu, "Graphene plasmonic metasurfaces to steer infrared light," *Sci. Rep.*, vol. 5, no. 1, Jul. 2015, Art. no. 12423.
[28] H.-Y. Chang *et al.*, "Large-area monolayer MoS_2 for flexible low-power RF nanoelectronics in the GHz regime," *Adv. Mater.*, vol. 28, no. 9, pp. 1818–1823, 2016.
[29] M. Grätzel, "The light and shade of perovskite solar cells," *Nat. Mater.*, vol. 13, no. 9, pp. 838–842, Sep. 2014.
[30] C. A. Randall, A. S. Bhalla, T. R. Shrout, and L. E. Cross, "Classification and consequences of complex lead perovskite ferroelectrics with regard to B-site cation order," *J. Mater. Res.*, vol. 5, no. 4, pp. 829–834, Apr. 1990.
[31] Y. Yamada, T. Nakamura, M. Endo, A. Wakamiya, and Y. Kanemitsu, "Photocarrier recombination dynamics in perovskite $CH_3NH_3PbI_3$ for solar cell applications," *J. Amer. Chem. Soc.*, vol. 136, no. 33, pp. 11610–11613, Aug. 2014.
[32] C. La-o Vorakiat *et al.*, "Elucidating the role of disorder and free-carrier recombination kinetics in $CH_3NH_3PbI_3$ perovskite films," *Nat. Commun.*, vol. 6, no. 1, p. 7903, Jul. 2015.
[33] M. A. Green, A. Ho-Baillie, and H. J. Snaith, "The emergence of perovskite solar cells," *Nat. Photon.*, vol. 8, no. 7, pp. 506–514, Jul. 2014.
[34] Y. Zhao and K. Zhu, "CH_3NH_3Cl-assisted one-step solution growth of $CH_3NH_3PbI_3$: Structure, charge-carrier dynamics, and photovoltaic properties of perovskite solar cells," *J. Phys. Chem. C*, vol. 118, no. 18, pp. 9412–9418, May 2014.
[35] S. K. Kurtz, J. R. Hardy, and J. W. Flocken, "Structural phase transitions, ferroelectricity and high temperature superconductivity," *Ferroelectrics*, vol. 87, no. 1, pp. 29–40, Nov. 1988.
[36] M. Tonouchi, "Cutting-edge terahertz technology," *Nat. Photon.*, vol. 1, no. 2, pp. 97–105, Feb. 2007.
[37] M. Shur, "Terahertz technology: Devices and applications," in *Proc. IEEE 31st Eur. Solid-State Circuits Conf. (ESSCIRC)*, Grenoble, France, 2005, pp. 13–22.
[38] A. Woessner *et al.*, "Highly confined low-loss plasmons in graphene–boron nitride heterostructures," *Nat. Mater.*, vol. 14, no. 4, pp. 421–425, Apr. 2015.
[39] L. L. Zhang and X. S. Zhao, "Carbon-based materials as supercapacitor electrodes," *Chem. Soc. Rev.*, vol. 38, no. 9, p. 2520, 2009.
[40] A. Alomainy, K. Yang, M. A. Imran, X.-W. Yao, and Q. H. Abbasi, Eds., *Nano-Electromagnetic Communication at Terahertz and Optical Frequencies: Principles and Applications*. London, U.K.: Inst. Eng. Technol., Nov. 2019.
[41] A. Abohmra, H. Abbas, S. F. Jilani, A. Alomainy, M. A. Imran, and Q. H. Abbasi, "High bandwidth perovskite based antenna for high-resolution biomedical imaging at terahertz," in *Proc. IEEE Int. Symp. Antennas Propag. USNC-URSI Radio Sci. Meeting*, Atlanta, GA, USA, Jul. 2019, pp. 503–504.
[42] L. Li, "Ferroelectric/superconductor heterostructures," *Mater. Sci. Eng. R, Rep.*, vol. 29, no. 6, pp. 153–181, Nov. 2000.
[43] M. Manjappa, Y. K. Srivastava, A. Solanki, A. Kumar, T. C. Sum, and R. Singh, "Hybrid lead halide perovskites for ultrasensitive photoactive switching in terahertz metamaterial devices," *Adv. Mater. (Deerfield Beach, Fla.)*, vol. 29, no. 32, Aug. 2017, Art. no. 1605881.
[44] L. Cong, Y. K. Srivastava, A. Solanki, T. C. Sum, and R. Singh, "Perovskite as a platform for active flexible metaphotonic devices," *ACS Photon.*, vol. 4, no. 7, pp. 1595–1601, Jul. 2017.
[45] A. Kumar *et al.*, "Excitons in 2D perovskites for ultrafast terahertz photonic devices," *Sci. Adv.*, vol. 6, no. 8, Feb. 2020, Art. no. eaax8821.
[46] J. Zhou *et al.*, "Ultrasensitive polarization-dependent terahertz modulation in hybrid perovskites plasmon-induced transparency devices," *Photon. Res.*, vol. 7, no. 9, pp. 994–1002, Sep. 2019.
[47] H. J. Snaith *et al.*, "Anomalous hysteresis in perovskite solar cells," *J. Phys. Chem. Lett.*, vol. 5, no. 9, pp. 1511–1515, 2014.
[48] C. C. Stoumpos, C. D. Malliakas, and M. G. Kanatzidis, "Semiconducting tin and lead iodide perovskites with organic cations: Phase transitions, high mobilities, and near-infrared photoluminescent properties," *Inorg. Chem.*, vol. 52, no. 15, pp. 9019–9038, 2013.
[49] E. T. Hoke, E. L. Unger, K. Vandewal, and M. D. McGehee, "Charge recombination and transport in hybrid perovskite solar cells: Why do perovskite solar cells have large Voc," in *Proc. MRS Fall Meeting Exhibit*, 2013, pp. 74–75.
[50] A. Abohmra *et al.*, "Low-profile flexible perovskite based millimetre wave antenna," in *Proc. IEEE MTT-S Int. Microw. Biomed. Conf. (IMBioC)*, vol. 1. Nanjing, China, May 2019, pp. 1–4.
[51] C. A. Balanis, Ed., *Modern Antenna Handbook*, 1st ed. New York, NY, USA: Wiley, Aug. 2008.
[52] J.-S. Hong and M. J. Lancaster, *Microstrip Filters for RF/Microwave Applications*. New York, NY, USA: Wiley, Jun. 2001.